

# HIGH MOMENTUM COMPONENTS OF NUCLEON MOMENTUM DISTRIBUTIONS EMERGING FROM SKYRME-HARTREE-FOCK CALCULATIONS

M.V. Stoitsov

*Institute for Nuclear Research and Nuclear Energy,  
Bulgarian Academy of Sciences, Sofia 1784, Bulgaria*

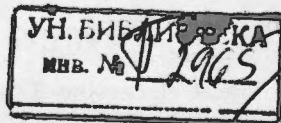
Received 19 July 1991

**Abstract.** The ability of the Skyrme-Hartree-Fock theory to reproduce the nucleon momentum distributions in a spherical nuclei is investigated systematically. The interest is also to state more quantitatively how the effective nucleon-nucleon forces contribute to the high-momentum region of nucleon momentum distributions including a comparison between different Skyrme-type forces. The results give useful preliminary information about the high-momentum components that are important in analyzing the data from inclusive hadron (pion and proton) and electron scattering experiments.

**Резюме.** Исследуется возможность применимости теории Хартри-Фока с силами Скирма в описании импульсных распределений нуклонов в сферических ядрах. Определено, что зависящие от плотности эффективные взаимодействия могут в основном учесть корреляции в области высоких передаваемых импульсов. Этот эффект не зависит существенно от выбора сил, которые неплохо воспроизводят другие характеристики основных состояний ядер. Результаты теории Хартри-Фока с силами Скирма представляют исключительно полезную информацию в области высоких передаваемых импульсов, что очень важно для обработки данных по инклюзивным адронным (пион-протонным) и электронным экспериментам.

## 1. Introduction

The high-momentum components of the nucleon momentum distribution  $n(k)$  contain valuable information about the nucleon correlations in nuclei [1-4]. For this reason, efforts are continuously devoted to determinate  $n(k)$  through inclusive hadron or electronic scattering experiments [5-10]. In contrast to the local density distribution  $\rho(r)$ , however, the nucleon momentum distribution  $n(k)$  is not directly



92

related to some observable quantities. One is therefore forced to make theoretical assumptions in order to extract  $n(k)$  from the measured experimental data. It is obviously desirable to have a simple enough but well justified theoretical model for handling the nucleon momentum distribution in nuclei.

An extensive review of the present momentum distribution calculations shows [11] that beyond  $2 \text{ fm}^{-1}$  the momentum distribution  $n(k)$  is dominated by the correlation effects. One has in mind rather involved approaches such as the coupled-cluster (or  $\exp(S)$ ) approach [1], the Brueckner-Bethe-Goldstone method [12] or the Jastrow method [2, 3]. In the lowest order, these approaches assume an uncorrelated nuclear ground state which corresponds to a single Slater determinant wave function (the Hartree-Fock model). However the single-particle wave functions  $\{\varphi_i\}$  are usually taken from the harmonic oscillator with a length parameter adjusted to fit the nuclear mean-squared charge radius. The high-momentum components in such a Slater determinant are small. The same is true also for a more sophisticated choice for  $\{\varphi_i\}$  whereby the single-particle set  $\{\varphi_i\}$  satisfies self-consistent Brueckner-Hartree-Fock [12] or generalized Brueckner-Hartree-Fock [1] equations. The high-momentum components of  $n(k)$  can emerge only in higher orders of the approaches [1-3, 12].

The situation differs in the case of density dependent Hartree-Fock calculations where the nucleon correlations are partially taken into account by means of the effective nucleon-nucleon interaction. The aim of the present paper is therefore to analyze systematically the high-momentum region of nucleon momentum distributions emerging from the density-dependent Hartree-Fock calculations. This will point out once more the particular status of the Skyrme (or, more generally, the density-dependent) Hartree-Fock formalism in handling the nucleon correlations in nuclei. For this purpose, we use throughout the work the Skyrme-type effective forces which provide a quite realistic mean-field description of the nuclear ground state [13].

The formal basis of the calculations is summarized in Section 2, the results in Section 3 and the conclusion in Section 4.

## 2. Effective Forces Formalism

In order to clarify the Skyrme-Hartree-Fock (SHF) calculations, let us introduce the concept of the effective forces in nuclei [14]. The correlated many-particle wave function  $\Psi \equiv \Psi(r_1, r_2, \dots, r_A)$  satisfies the exact Schrödinger equation

$$\hat{H}\Psi(r_1, r_2, \dots, r_A) = E\Psi(r_1, r_2, \dots, r_A) \quad (1)$$

where the lowest eigenvalue  $E$  is the exact ground-state energy of the system of  $A$  nucleons with Hamiltonian  $H$ . The correlated function  $\Psi$  factorizes into both the single Slater determinant  $\Phi \equiv \Phi(r_1, r_2, \dots, r_A) = (A!)^{-1/2} \det |\varphi_i(r_j)|$  and the operator  $F_{\text{corr}}$  which takes the correlations into account

$$\Psi(r_1, r_2, \dots, r_A) = \hat{F}_{\text{corr}}\Phi(r_1, r_2, \dots, r_A). \quad (2)$$

The many-body problem (1) then becomes a Hartree-Fock problem

$$\hat{H}_{\text{eff}}\Phi(r_1, r_2, \dots, r_A) = E\Phi(r_1, r_2, \dots, r_A) \quad (3)$$

with effective Hamiltonian

$$H_{\text{eff}} = \hat{F}_{\text{corr}}^+ \hat{H} \hat{F}_{\text{corr}} \quad (4)$$

where  $\hat{F}_{\text{corr}}^+ = (\hat{F}_{\text{corr}})^{-1}$ .

Suppose that the effective Hamiltonian (4) is known. Then the solution  $\{\varphi_i\}$  of the Hartree-Fock problem is obviously affected by the correlations entering the effective Hamiltonian  $H_{\text{eff}}$ . For any observable  $A$  one should construct, analogously to Eq. (4), the associated effective operator.

$$\hat{A}_{\text{eff}} \equiv \hat{F}_{\text{corr}}^+ \hat{A} \hat{F}_{\text{corr}} = \hat{A} + \Delta \hat{A}_{\text{eff}}, \quad (5)$$

which normally defines  $\Delta \hat{A}_{\text{eff}}$ . Obviously, the use of the effective Hamiltonian (4) affects both parts of the observable

$$A \equiv \langle \Psi | \hat{A} | \Psi \rangle \equiv \langle \Phi | \hat{A}_{\text{eff}} | \Phi \rangle = \langle \Phi | \hat{A} | \Phi \rangle - \langle \Phi | \Delta \hat{A}_{\text{eff}} | \Phi \rangle. \quad (6)$$

The first part  $\langle \Phi | \hat{A} | \Phi \rangle$  is affected by the correlations through the particular set  $\{\varphi_i\}$  satisfying Eq. (3) and building up the Slater determinant  $|\Phi\rangle$ . The second part  $\langle \Phi | \Delta \hat{A}_{\text{eff}} | \Phi \rangle$  additionally depends on the particular form of the operator  $\hat{F}_{\text{corr}}$ . All above expressions are obviously exact.

The SHF assumption consists in the following: the Skyrme-type effective forces in nuclei directly parameterize the effective Hamiltonian (4). Fitting the free parameters of the forces to the measured data the SHF calculations give, at least in principle, the exact ("correlated") single particle set  $\{\varphi_i\}$  thus avoiding the enormous problem of evaluating the operator  $F_{\text{corr}}$ . However, since the operator  $\hat{F}_{\text{corr}}$  is not known, a second assumption requires only the normal operators  $\hat{A}$  in Eq. (5) to be used in the SHF calculations. As a result, the SHF model takes into account only the first part  $\langle \Phi | \hat{A} | \Phi \rangle$  of the observable (6). In particular, the following SHF expressions are taken for the local density distribution

$$\rho(r) = \sum_{i=1}^A |\varphi_i(r)|^2 \quad (7)$$

and the nucleon momentum distribution

$$n(k) = \sum_{i=1}^A |\bar{\varphi}_i(k)|^2 \quad (8)$$

where  $\bar{\varphi}_i(k)$  is the Fourier transform of  $\varphi_i(r)$ .

In other words, the SHF model uses effective density-dependent forces but only the normal operators  $\hat{A}$  which is obviously acceptable for those observables that are not much affected by the correlation factor  $F_{\text{corr}}$ . One has particularly in mind the local density distribution [15], the low momentum components of the associated form factors and the bulk properties of nuclei [13]. In this respect, the ability of the SHF model to reduce the high-momentum components of  $n(k)$  may be questioned because the operator  $F_{\text{corr}}$  is expected to play a crucial role at high-momentum transfers where the short-range correlations and the mesonic

degrees of freedom become important [14]. An adequate theoretical framework there should include approaches [1-3, 12] which take the complete transformation (5) into account. Nevertheless, due to the widespread use of the SIIF theory, it is important to analyze to what extent this theory is able to reproduce the nucleon momentum distribution in nuclei.

### 3. Results

We have carried out SIIF calculations with the five sets of Skyrme-type force parameters listed in Table 1.

Table 1. Different sets of parameters of Skyrme-type effective forces used and the associated infinite nuclear matter characteristics

Force	Parameters									
	$t_0$	$t_1$	$t_2$	$t_3$	$W_0$	$x_0$	$x_1$	$x_2$	$x_3$	$\alpha$
SI	-1057.30	235.90	-100.00	14463.5	120	0.560	0.0	0.0	1.000	1
SIH	-1128.75	395.00	-95.00	14000.0	120	0.450	0.0	0.0	1.000	1
SV	-1248.29	970.56	107.22	0.0	150	-0.170	0.0	0.0	1.000	1
T1	-1794.00	298.00	-298.00	12812.0	110	0.154	-0.5	-0.5	0.089	1/3
SkM*	-2645.00	410.00	-135.00	15595.0	130	0.090	0.0	0.0	0.000	1/6

Force	Nuclear matter characteristics					
	$\rho_0, \text{fm}^{-3}$	$k_F^0, \text{fm}^{-1}$	$E_{NM}/N, \text{MeV}$	$K_{NM}/N, \text{MeV}$	$\alpha_r, \text{MeV}$	$(m^*/m)$
SI	0.15536	1.32	-16.000	370.0	29.3	0.91
SIH	0.14530	1.29	-15.870	355.4	28.16	0.76
SV	0.15536	1.32	-16.060	306.0	32.72	0.38
T1	0.16100	1.336	-15.980	236.1	32.02	1.00
SkM*	0.16030	1.334	-15.776	216.7	30.03	0.79

The values are taken as follows: SI from [20], SIH and SV from [18], T1 from [22] and SkM\* from [21]. The units are: MeV fm<sup>3</sup> for  $t_1$ , MeV fm<sup>5</sup> for  $t_1, t_2, W_0$  and MeV fm<sup>3+3 $\alpha$</sup>  for  $t_3$ .

Although the associated nuclear matter characteristics (Table 1) are quite different, all forces used lead to nearly the same SIIF description of the nuclear ground state [14]. The use of different Skyrme-type forces is expected to reveal also the sensitivity of the results for  $n(k)$  from the characteristics of the nuclear effective forces.

The SIIF momentum description (8) for the nucleus <sup>16</sup>O calculated with SIH (full line) and SkM\* (dashed line) forces are compared in Fig. 1 with the momentum distributions RSC and SSCB calculated by the coupled cluster approach [1] with Reid soft-core and de Tourreii-Sprung super soft-core B potentials, respectively. The momentum distribution H0, calculated with the harmonic oscillator shell model wave functions which is close to the uncorrelated results (UNC) following from the lowest order (generalized Brueckner-Hartree-Fock) of the coupled-cluster approach [1] is also shown in Fig. 1.

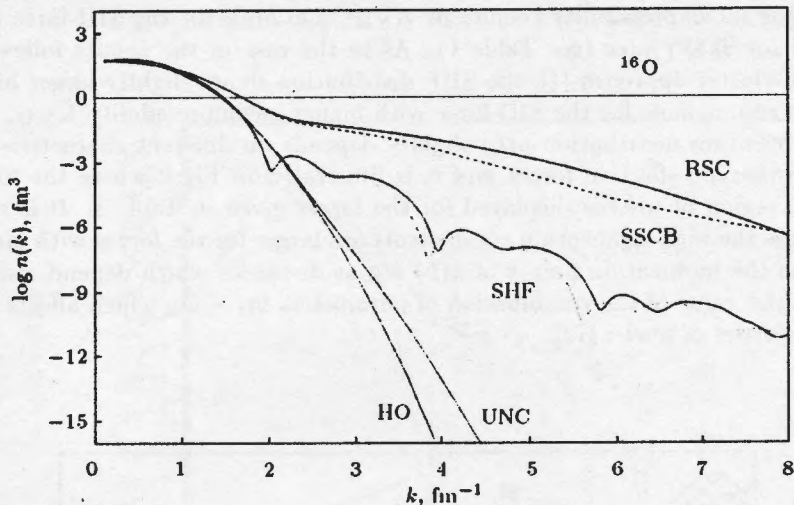


Fig. 1. The nucleon momentum distributions for the nucleus  $^{16}\text{O}$ . Coupled-cluster approach calculations [1], RSC: Reid soft-core potential, SSCB: de Tourreil-Sprung super soft-core potential B, UNC: uncorrelated results for the RSC potential. Skyrme-Hartree-Fock (SHF) results are obtained with SIII-force (full line) and SkM $^*$ -force (dashed line). The momentum distribution HO is calculated with harmonic oscillator wave functions. Throughout the work the normalization of  $n(k)$  is  $\int n(k)k^2dk = A$ .

It becomes clear (Fig. 1) that the momentum distributions considered are nearly the same in the inner region (up to  $k \approx 1 \text{ fm}^{-1}$  where the Pauli correlations are mainly important). This means that neither the particular form of the single-particle set  $\{\varphi_i\}$  nor the operator  $F_{\text{corr}}$  affects the low momentum region of the nucleon momentum distribution  $n(k)$ . Therefore, as already mentioned in [12, 16], the SHF theory is completely adequate in describing the inner region of  $n(k)$ .

At momenta above  $2 \text{ fm}^{-1}$ , the correlated distributions RSC and SSCB show significant high-momentum components in contrast with the uncorrelated HO distribution. Obviously, the "correlated" basis  $\{\varphi_i\}$  as well as the operator  $F_{\text{corr}}$  are both important in this region. Although, as remarked in [2, 3, 17], a single Slater determinant is not able to reproduce completely the form factor and  $n(k)$  of a correlated system, Fig. 1 shows that the SHF momentum distribution effectively takes into account a definite part of the nucleon correlations through the particular form of the "correlated" single-particle wave functions  $\{\varphi_i\}$ . The SHF results are still about four orders of magnitude lower than the correlated (RSC and SSCB), but many orders of magnitude higher than the uncorrelated (HO) results for almost all values of  $k \geq 3 \text{ fm}^{-1}$ . The SHF momentum distribution shows an oscillatory behaviour at above  $\approx 2 \text{ fm}^{-1}$  which reflects the finite range of the self-consistent SHF potential. This extra structure of the SHF results is obviously obscured by the correlations  $\hat{F}_{\text{corr}}$ .

It's worth mentioning the slight dependence of the high-momentum region of  $n(k)$  with respect to particular characteristics of the effective forces used. Both SHF

curves in Fig. 1, for example, correspond to Skyrme-type forces with quite different values for the incompressibility coefficient  $K_{NM}$ : 356 MeV for the SIII-force and 216.7 MeV for SkM\* force (see Table 1). As in the case of the results following the coupled-cluster approach [1], the SIF distribution shows slightly larger high-momentum components for the SIII-force with higher incompressibility  $K_{NM}$ .

The momentum distribution  $n(k)$  slightly depends on different characteristics of the Skyrme-type effective forces and it is illustrated in Fig.2 where the high-momentum region of  $n(k)$  is displayed for the forces given in Table 1. It is seen that as a rule the high-momentum components are larger for the forces with larger  $K_{NM}$ . Also the momentum points of  $n(k)$  are at distances which depend almost linearly on the value of the combination of parameters  $9t_1 - 5t_2$  which affects the surface properties of nuclei [18].

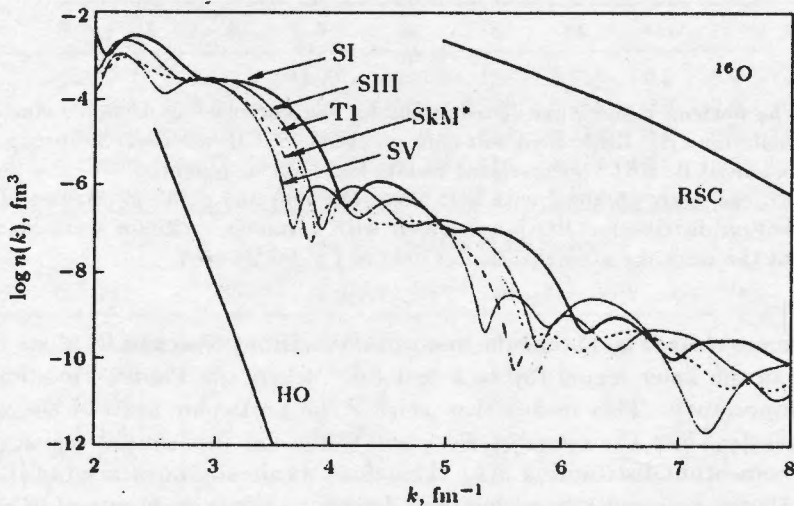


Fig. 2. The high-momentum tails of the SIF momentum distributions  $n(k)$  calculated for  $^{16}\text{O}$  with the Skyrme-type forces given in Table 1. The momentum distributions RSC and HO are the same as in Fig. 1

The knowledge of high-momentum components of the SIF momentum distribution, even having in mind the defect of the partial description of the nucleon correlations, is nevertheless important in the light of the fact that at present the experimental data still give no unique information about the momentum distribution of nuclei. For example, the SIF results for the momentum distributions of  $1p_{1/2}$ - and  $1p_{3/2}$ -shell protons in  $^{16}\text{O}$  agree with the available experimental data as shown in Figs 3 and 4, respectively. In this case, the fully correlated momentum distribution [1] has obviously too large high-momentum tail. However, the comparison with recent experimental data for  $n(k)$  in  $^{12}\text{C}$  (Fig. 5) supports just the opposite conclusion.

A knowledge of the high-momentum region of the SIF momentum distribu-

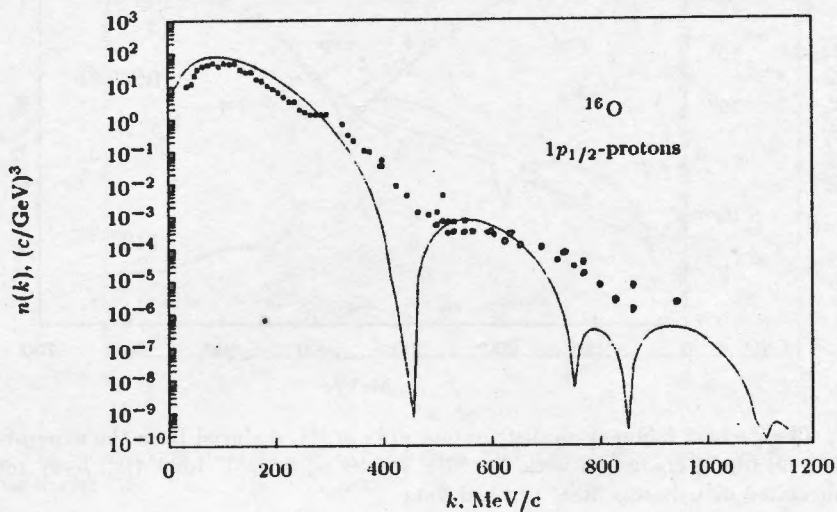


Fig. 3. The momentum distributions of  $p_{1/2}$ -shell protons on  $^{16}\text{O}$  from the data [23] of the  $(e, e', p)$  and  $(\gamma, p_0)$  reactions (dots) compared with SIF results (full line) obtained with SkM<sup>\*</sup>-force

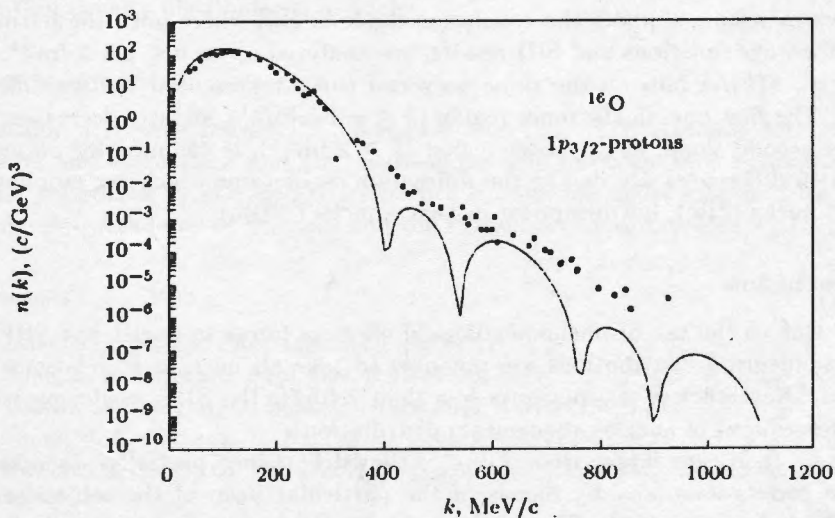


Fig. 4. The momentum distributions of  $p_{3/2}$ -shell protons on  $^{16}\text{O}$  from the data [23] of the  $(e, e', p)$  and  $(\gamma, p_0)$  reactions (dots) compared with SIF results (full line) obtained with SkM<sup>\*</sup>-force

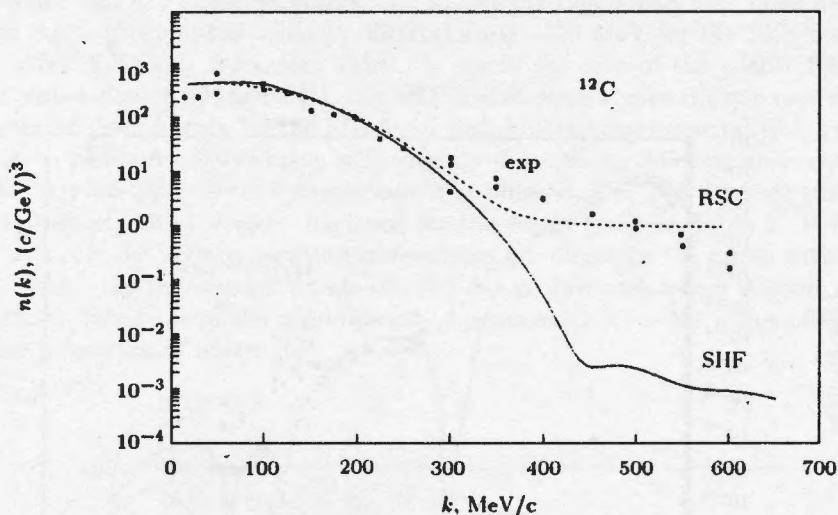


Fig. 5. The nucleon momentum distribution  $n(k)$  in  $^{12}\text{C}$  deduced from the experimental data [10, 19] (dots) compared with the SIIF results with SkM\*-force (full line) and the fully correlated distribution RSC (dashed line)

tion is also important as preliminary information for nuclei where complicated approaches [1-3, 12] are practically impossible for applications. As an example for the SIIF nucleon momentum distributions for the set of nuclei  $^4\text{He}$ ,  $^{16}\text{O}$ ,  $^{40}\text{Ca}$ ,  $^{90}\text{Zr}$  and  $^{208}\text{Pb}$  calculated with SkM\*-force are shown in Fig. 6. It is seen that the present results support the conclusion made in [16] where both the harmonic oscillator wave functions and SIIF results, are analyzed up to  $k \leq 1.5\text{-}2 \text{ fm}^{-1}$ . For all nuclei,  $n(k)/A$  falls on the same universal curve represented by two different slopes. The first one, in the inner region ( $k \leq 1\text{-}1.5 \text{ fm}^{-1}$ ), slightly decreases with  $A$ . The second slope, in the outer region ( $k \geq 2 \text{ fm}^{-1}$ ), is common for all nuclei. The main differences are due to the diffraction oscillations which are emphasized in light nuclei ( $^4\text{He}$ ), but disappear in heavy nuclei ( $^{208}\text{Pb}$ ).

#### 4. Conclusion

(1) Due to the use of phenomenological effective forces in nuclei, the SIIF nucleon momentum distributions are not able to take all nucleon correlations into account. Nevertheless, at momenta less than  $2 \text{ fm}^{-1}$ , the SIIF results provide a good description of nucleon momentum distributions.

(2) At momenta larger than  $2 \text{ fm}^{-1}$ , the SIIF theory partially accounts for nuclear correlations only by means of the particular form of the self-consistent single-particle states  $\{\varphi_i\}$ . The SIIF results for the high-momentum tail of  $n(k)$  are lower than the associated values of the fully correlated momentum distribution, but they are many orders of magnitude higher than the uncorrelated results.

(3) For all nuclei,  $n(k)/A$  falls on the same universal curve which is almost independent of the particular set of Skyrme-type forces used. The main differences in the high-momentum region are due to the nonmonotonic behaviour of  $n(k)$  which

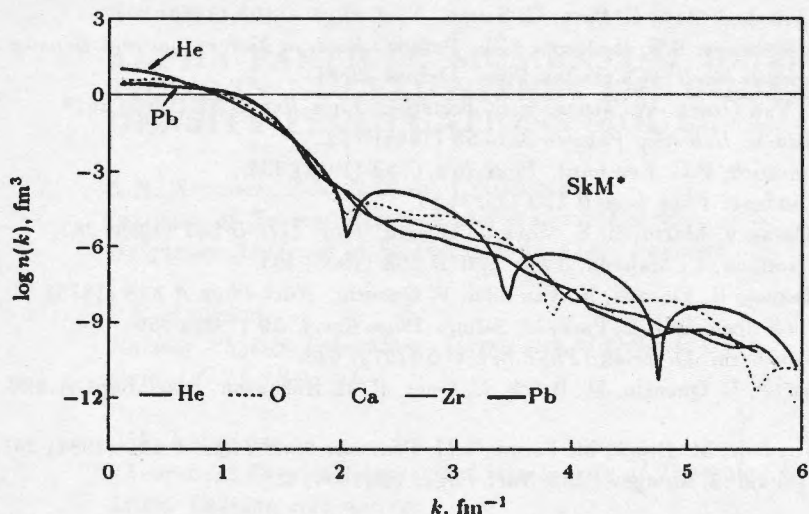


Fig. 6. The momentum distribution  $n(k)/A$  from SHF calculations with SkM\*-force for the set of nuclei  ${}^4\text{He}$ ,  ${}^{16}\text{O}$ ,  ${}^{40}\text{Ca}$ ,  ${}^{90}\text{Zr}$  and  ${}^{208}\text{Pb}$

disappears with increasing  $A$  and which is completely obscured by the correlations.

(4) In the light of the wide range of contemporary applications of the SHF theory and the quite crude experimental determination of  $n(k)$ , the SHF results give useful preliminary information about the high-momentum region of nucleon momentum density distributions in nuclei.

### Acknowledgments

The author acknowledges Dr. P.E. Hodgson and Dr. A.N. Antonov for helpful comments and discussions and Dr. Slimane for help in computing. This work is partially supported by the Bulgarian Science Committee under Contract No 325, the Bulgarian Academy of Sciences and the Royal Society of London.

### References

- 1 G. Zabolitzky, W. Ey. *Phys. Lett. B* **76** (1978) 527.
- 2 O. Bohigas, S. Stringari. *Phys. Lett. B* **95** (1980) 9.
- 3 M. Dal Ri, S. Stringari, O. Bohigas. *Nucl. Phys. A* **370** (1982) 81.
- 4 M. Jaminon, C. Mahaux, H. Ngo. *Nucl. Phys. A* **452** (1986) 445.
- 5 S. Frankel, W. Frati, O. Van Dyck, R. Werbeck, V. Highland. *Phys. Rev. Lett.* **36** (1976) 642.
- 6 R. Amado, R.M. Woloshyn. *Phys. Rev. Lett.* **36** (1976) 1435.
- 7 D. Day, J.S. McCarthy, Z.E. Meziani, R. Minehart, R. Sealock, S. Sealock, S.T. Thornton, J. Jourdan, I. Sick, B.W. Filippone, R.D. McKeown, R.G. Milner, D.H. Potterveld, Z.W. Szalata. *Phys. Rev. Lett.* **59** (1987) 427.
- 8 D. Day, J.S. McCarthy, I. Sick, R.G. Arnold, B.T. Chertok, S. Rock, Z.M. Szalata, F. Martin, B. Mecking, G. Tamas. *Phys. Rev. Lett.* **43** (1979) 1143.



- 9 Ji Xiangdong, J. Engel. *Phys. Rev. C* **40** (1989) R497.
- 10 C. Ciofi degli Atti, E. Pace, G. Salmè. *Nucl. Phys. A* **495** (1989) 361.
- 11 A.N. Antonov, P.E. Hodgson, I.Zh. Petkov. *Nucleon Momentum and Density Distributions in Nuclei* (Clarendon Press, Oxford 1988).
- 12 J.W. Van Orden, W. Truex, M.K. Banerjee. *Phys. Rev. C* **21** (1980) 2628.
- 13 M. Brack. *Helvetica Physica Acta* **58** (1985) 715.
- 14 J. Friedrich, P.G. Reinhard. *Phys. Rev. C* **33** (1986) 335.
- 15 F. Tondeur. *Phys. Lett. B* **123** (1983) 13.
- 16 M. Casas, J. Martorell, E. Moya de Guerra. *Phys. Lett. B* **167** (1986) 263.
- 17 M. Jaminon, C. Mahaux. *Phys. Lett. B* **158** (1985) 103.
- 18 M. Beiner, H. Flocard, N. Van Giai, P. Quentin. *Nucl. Phys. A* **238** (1975) 29.
- 19 C. Ciofi degli Atti, E. Pace, G. Salme. *Phys. Rev. C* **39** (1989) 259.
- 20 D. Vautherin, D. Brink. *Phys. Rev. C* **5** (1972) 626.
- 21 J. Bartel, P. Quentin, M. Brack, C. Guet, H.-B. Håkanson. *Nucl. Phys. A* **386** (1982) 79.
- 22 F. Tondeur, M. Brack, M. Farine, J.M. Pearson. *Nucl. Phys. A* **420** (1984) 297.
- 23 S. Frullani, J. Mougey. *Adv. Nucl. Phys.* **14** (1984) 1.